IEEE Access
Multidisciplinary | Rapid Review | Open Access Journal

Received April 27, 2019, accepted May 15, 2019, date of publication May 22, 2019, date of current version June 5, 2019.

Digital Object Identifier 10.1109/ACCESS.2019.2918277

An Adaptive Equivalent Consumption Minimization Strategy for Plug-In Hybrid Electric Vehicles Based on Energy Balance Principle

YONGGANG LIU[1], (Senior Member, IEEE), JIE LI[1], ZHENZHEN LEI[1], (Member, IEEE), WENZHI LI[1], DATONG QIN[1], AND ZHENG CHEN[2], (Senior Member, IEEE)

[1]State Key Laboratory of Mechanical Transmissions, School of Automotive Engineering, Chongqing University, Chongqing 400044, China
[2]Faculty of Transportation Engineering, Kunming University of Science and Technology, Kunming 650500, China

Corresponding authors: Zhenzhen Lei (2010048@cqust.edu.cn) and Zheng Chen (chen@kmust.edu.cn)

This work was supported in part by the National Natural Science Foundation of China under Grant 61763021and Grant 51775063, in part by the National Key R&D Program of China under Grant 2018YFB0104000 and Grant 2018YFB0104900, in part by the Fundamental Research Funds for the Central Universities under Grant 2018CDQYQC0035, and in part by the EU-Funded Marie Skłodowska-Curie Individual Fellowships Project under Grant 845102-HOEMEV-H2020-MSCA-IF-2018.

ABSTRACT Energy management strategies can directly determine the dynamic performance and fuel economy of plug-in hybrid electric vehicles (PHEVs). In this paper, an adaptive equivalent consumption minimization strategy (A-ECMS) is proposed based on the energy balance principle of the hybrid powertrain of the target vehicle, by which a pair of boundary equivalent factors can be determined according to the future transportation information. Then, the equivalent factor is calculated in real time based on the energy variation in the powertrain system during the operation. Consequently, the torque distribution between the engine and the motor can be determined by solving the Hamilton function according to the dynamically adjusted equivalent factor, and thus, the energy management control is adaptively realized. The simulations were conducted considering three typical driving conditions, different battery aging statuses, and inaccurate road information. The results manifest that the proposed algorithm is feasible to improve the fuel economy with attainable adaptivity and robustness compared with the typical ECMS.

INDEX TERMS Plug-in hybrid electric vehicles (PHEVs), adaptive equivalent fuel consumption minimum strategy (A-ECMS), energy balance principle, equivalent factor, probability factor.

I. INTRODUCTION

As a combination of electric drive and traditional engine drive, hybrid electric vehicles (HEVs) can effectively reduce fuel consumption and exhaust emissions, compared to internal combustion engine (ICE) vehicles [1]. With the development of battery technologies, plug-in HEVs (PHEVs) not only incorporate all functions and merits of HEVs, but also can supply a certain all-electric range (AER) powered by the built-in battery pack [2]. Since PHEVs contain at least two energy sources, usually the engine and battery, an indispensable control problem arises that the power distribution between these two energy sources needs to be properly dealt with, referred to as the energy management [3]. An efficient energy management for PHEVs cannot only improve the fuel economy with the premise of satisfying the driving power demand, but also extend the battery lifetime and reduce the emissions.

Nowadays, a variety of research has been conducted for energy management strategies of PHEVs. Usually, they can be mainly divided into two categories: 1) rule-based strategies, and 2) optimization-based strategies [4]. For the rule-based strategy, as its name implies, a most important task is to design an effective rule table, which usually requires enough development experience. In this case, trial-and-error iterations are often conducted trying to control the engine working in the most efficient region, thereby gaining the desired controlling efficiency [5], [6]. Finally, a pre-defined rule table can be generated to control the energy distribution according to the vehicle powertrain status including the

The associate editor coordinating the review of this manuscript and approving it for publication was Arup Kumar Goswami.

2169-3536 © 2019 IEEE. Translations and content mining are permitted for academic research only.
Personal use is also permitted, but republication/redistribution requires IEEE permission.
See http://www.ieee.org/publications_standards/publications/rights/index.html for more information.

engine, battery, and power demand [7]. A typical rule-based strategy is the charge depletion/charge sustaining (CD/CS) scheme, which is widely adopted by vehicle manufacturers. Usually, the rule-based method does not take into account the system's dynamic characteristics and relies much on previous engineering experience [8]. From this point of view, it is difficult for rule-based algorithms to find an optimal solution effectively and a variety of design intensity and repetitive iteration is necessary to improve the controlling performance.

For optimization-based strategies, investigators usually utilize them to find the optimal or quasi-optimal solutions. One type of these strategies is based on intelligent algorithms that need a series of training actions [9]. Popular solutions include neural networks (NN) [10], [11], genetic algorithm (GA) [12], simulated annealing (SA) algorithm [13], particle swarm optimization (PSO) [14], etc. For these types of methods, one main constraint is that they all need the detailed trip information, which is difficult to acquire in real application. Another point is that they rely on a variety of optimal operation data, which should be obtained by other optimization algorithms. Different from rule-based strategies, these methods usually train the control model as a black box with a variety of offline data and typical driving conditions. No doubt, they are cost-effective, time-consuming, and demand intensive computation labor and considerable storage space.

Another type of optimization-based algorithms is mainly based on the optimal theory and can be divided into two categories: global optimization algorithms and instantaneous optimization methods. Global optimization algorithms can be dynamic programming (DP) [11], convex optimization [15], quadratic programming (QP) [3], [16], and linear programming. These algorithms can find the global optimal solution given prior knowledge of driving conditions [5]–[9]. They are usually regarded as the benchmark for evaluating other strategies' performance. DP is firstly adopted to achieve the energy distribution for a hybrid electric truck [17]. A main concern when applying DP is the induced intensive matrix computation, i.e., the so-called curse of dimensionality. Convex optimization can be applied to find the optimal energy distribution only if the vehicle model can be built as a single or multi convex functions [18]. QP can be applied to optimize the fuel economy if the fuel rate can be approximated with a series of quadratic equations [19]. In engineering applications, global optimization strategy lays a solid foundation for developing more feasible and real-time energy management strategies.

In contrast, instantaneous optimization strategies can consider transient characteristics of the motor and engine under different operating conditions in real time, thereby determining proper working modes of the hybrid system and achieving energy distribution. The most representative candidates belong to the equivalent consumption minimization strategy (ECMS) [20] and Pontryagin's minimum principle (PMP) [21], [22]. Both strategies are essentially the same and declare to find optimal solutions by solving the Hamilton function. The ECMS converts the current electric energy consumption into the future fuel consumption of the engine in an equivalent manner, and then calculates the minimum instantaneous equivalent fuel consumption, by which the optimal energy distribution ratio is decided [23]. The ECMS exhibits strong dynamic adaptability, which does not require prior knowledge of driving conditions and can theoretically achieve the optimal or near-optimal solutions, compared to DP. On this account, it has attracted wide attention from industry and academia that have make much effort to improve its controlling performances.

For the ECMS, a key problem is to estimate the equivalent factor timely and accurately, which can be obtained by solving a two-point boundary problem that consists of the Hamilton function, terminal cut-off conditions and corresponding constraints. Directly finding the solution is difficult and sometimes even impossible. Traditional way to obtain the optimal equivalent factor is achieved through simulation and experiment. These methods can be time consuming and yet the acquired equivalent factor can only be effective in a specific condition. They are difficult to adapt to real complex driving conditions. Currently, the most popular manner is to determine the optimal equivalent factor offline under different driving cycles, and then identify the driving condition online to choose appropriate values for real-time application [4], [24], [25]. This method is validated effective under a single driving condition; however, it usually cannot be qualified when the driving condition is highly mixed with different road types. Compared with the simple ECMS, the adaptive ECMS (A-ECMS) is more capable of managing energy distribution and improving fuel economy to some extent [26], [27]. In [28], [29], the A-ECMS is proposed by regulating the battery state of charge (SOC) based on linear or nonlinear control algorithms, such as the typical proportional-integral-differential (PID) controller. It can reduce correlation between the equivalent factor and driving condition, and only needs to calculate the difference between the current SOC and expected value. In this manner, dynamic adjustment of the equivalent factor can be tackled according to feedback of the SOC difference. However, this method takes the SOC error into account, and neglects influences induced by the battery capacity variation. Furthermore, with the development of global positioning system (GPS), graphical information system (GIS), and intelligent transportation system (ITS), more detailed transportation information can be acquired and possibly predicted in advance based on internet of vehicles (IOV) [30], by which the equivalent factor can be tuned dynamically. How to effectively make use of future transportation information to achieve adaptive regulation of the equivalent factor has become a research focus.

Considering the aforementioned problems and emerging technologies, in this study, a novel A-ECMS is proposed for the PHEV based on energy balance principle of the hybrid system, which can be easily applied during the charge sustaining (CS) stage of the vehicle. The strategy aims to improve the real-time controlling performance and reduce the

calculation complexity. In this paper, the proposed A-ECMS consists of two layers. In the upper layer, the energy balance model of the powertrain system is built and the relationship between the battery electric energy and fuel heat energy is determined. Meanwhile, the future transportation information needs to be acquired ahead of departure, and based on it, the variation range of the equivalent factor is defined by calculating a pair of boundary equivalent factors. The main function of the bottom layer is to determine the probability factor according to real-time energy variation during operation and regulate the equivalent factor adaptively based on the determined probability factor within the restrictions determined in the upper layer. Simulations were conducted under three typical driving cycles, i.e., the urban dynamometer driving schedule (UDDS), new European driving cycle (NEDC) and worldwide harmonized light vehicles test cycle (WLTC), to verify performance of the proposed strategy. Results manifest that the proposed algorithm can gain superior fuel savings under different driving conditions, compared to the typical ECMS. In addition, the proposed algorithm also takes the battery degradation into account. Simulation results show that when the battery is degraded, the savings can reach up to 12%, proving effectiveness and robustness of the proposed algorithm. Furthermore, simulation with inaccurate road information was also performed to validate the algorithm's adaptivity when faced with imprecise global driving information. The main contributions of this study can be attributed to the following two aspects: 1) A novel A-ECMS is proposed based on the energy balance principle of the hybrid powertrain system. The strategy can regulate the equivalent factor dynamically according to the driving condition and battery performance variation. Compared to the typical ECMS, generality and robustness of the strategy are obviously improved. 2) The energy balance model of the PHEV is built, and the transformation relationship is built between the battery power and engine power, by which it becomes easier to apply the proposed algorithm.

The remainder of this paper is organized as follows. Section II models the PHEV and powertrain components. In Section III, adaptive adjustment of the equivalent factor is introduced in detail. Section IV provides corresponding simulations and verifies feasibility of the proposed algorithm, followed by the main conclusion drawn in Section V.

II. PHEV MODEL AND CONFIGURATION

The vehicle studied in this paper is a parallel PHEV. The main powertrain topology is sketched in Fig. 1. It can be observed that there exists a clutch between the engine and integrated-starter-generator (ISG), and an automated manual transmission (AMT) is equipped between the ISG and final drive. The main parameters are listed in Table 1, where we can find that the maximum engine power is 105 kW and the maximum motor power is 52 kW. It can be intuitively judged that the engine occupies most of the power demand during the CS stage. The AMT has five gear ratios, i.e. 2.56/1.55/1.02/0.73/0.52, and can be shifted automatically

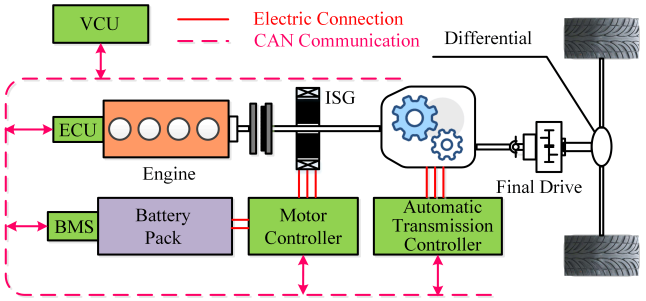

FIGURE 1. Structure of the PHEV powertrain system.

TABLE 1. Vehicle specifications.

Component	Value
Vehicle Type	Parallel PHEV
Vehicle	Front-wheel drive Mass 1720 kg
Engine	Maximum power 105 kW Maximum speed 6000 r/min Maximum torque 202 Nm
Motor	Rated power 35kW Maximum power 52 Kw Maximum torque 400 Nm
Transmission	5 speed AMT 2.56/1.55/1.02/0.73/0.52
Battery	Lithium-ion battery pack Serial number 72 Maximum power 61 kW Rated capacity 41 Ah Rated voltage of a single cell 3.6V

according to the speed and power demand, leading to easier design of the energy management strategy.

A. VEHICLE LONGITUDINAL DYNAMIC MODEL

In this study, the main target is to improve the fuel economy and maintain the SOC around the stable value under the CS mode. To achieve this target, the vehicle longitudinal dynamics model needs to be established,

$$P^{+}_{dem} = (mgf\cos\alpha + mg\sin\alpha + ma + 0.5C_D A\rho_a v^2)\cdot v \quad (1)$$

$$P^{+}_{dem} = \left(P^{+}_{mot} + P^{+}_{ice}\right)\bar{\eta}_m \quad (2)$$

where P^{+}_{dem} denotes the demanded power of the vehicle, P^{+}_{mot} means the output power of the motor, P^{+}_{ice} is the engine power. It is necessary to note that the superscripts $+$ and $-$ in this paper denote the default value of the variable is positive and negative, respectively. $\bar{\eta}_m$ means average efficiency of the mechanical transmission system. m expresses the vehicle mass, g is the gravity acceleration and equals 9.8 m/s^2, f presents the rolling coefficient, α is the slope of road, C_D expresses the drag coefficient, A is the frontal area and supposed to be 2.25 m^2, ρ_a is the air density, v is the vehicle speed, and a denotes the vehicle acceleration.

B. ENGINE MODEL

For the engine, the common modeling manner mainly includes the theoretical analysis, numerical simulation and experimental data fitting method. Since the engine is a high

nonlinear time-varying system, in this study, we adopt the experimental data fitting method to lessen computation burden without much influence on modeling precision. By interpolating the steady experimental data, the engine fuel rate and efficiency can be calculated as,

$$\dot{m}_f(t) = f\left(T_e(t), n_e(t)\right) \tag{3}$$

$$\eta_e = \frac{T_e(t) \cdot n_e(t)}{9550 \times \dot{m}_f(t) \cdot H_{LHV}} \tag{4}$$

where $\dot{m}_f(t)$ is the fuel rate, and n_e, $T_e$andη_e denote its speed, torque and efficiency, respectively. H_{LHV} is the lower heating value of the fuel and equals 44000 kJ/kg. Fig. 2 shows the engine fuel rate map with respect to different torque and speed. Fig. 3 shows the engine hot efficiency map, from which we can find that the maximum efficiency is greater than 35%.

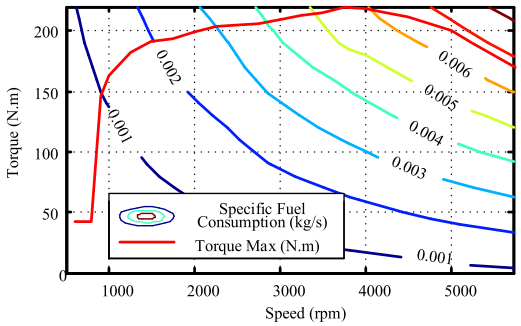

FIGURE 2. Engine fuel rate map.

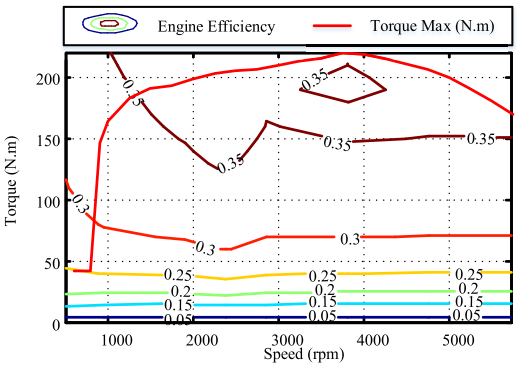

FIGURE 3. Engine efficiency model.

C. ELECTRICAL MOTOR MODEL

Similar to the engine modeling process, this study employs the experimental data fitting method to model the electrical motor. The motor's efficiency and speed characteristics can be acquired by interpolation of experimental data, as shown in Fig. 4, and it can be found that its highest efficiency is more than 90%.

D. BATTERY MODEL

In this study, an effective but simple battery model, which consists of a voltage source and a resistor connected in series,

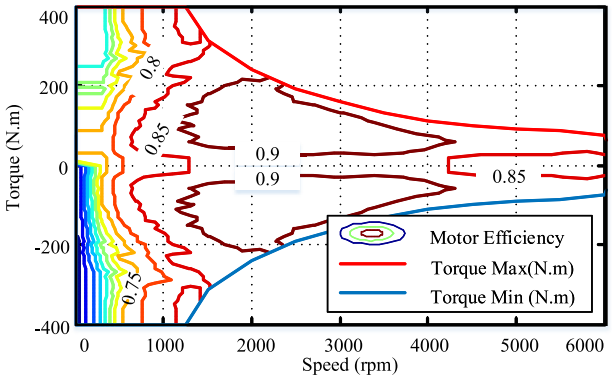

FIGURE 4. Electric motor efficiency map.

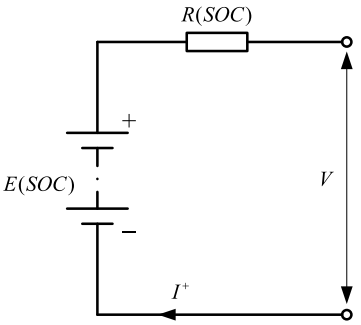

FIGURE 5. Battery model.

is adopted based on the experimental data and empirical formula, as shown in Fig. 5. As can be seen in Table 1, the rated voltage of the battery is 259 V and its rated capacity is 41 Ampere hour (Ah).

According to the Kirchhoff's voltage law, the current of the battery can be expressed as,

$$I^+(t) = \frac{E(SOC) - \sqrt{E(SOC)^2 - 4R(SOC)P^+(t)}}{2R(SOC)P^+(t)} \tag{5}$$

where $P^+(t)$ denotes the battery output power, $E(SOC)$ presents the open circuit voltage (OCV), $I^+(t)$ denotes the loop current, and $R(SOC)$ expresses the internal resistance. In addition, the battery SOC is a key control parameter when devising the energy management strategy. In this study, the coulomb counting method is employed to estimate the SOC, as:

$$SOC = SOC_0 - \frac{\int_{t0}^{t} I^+(t)dt}{C_{bat}} \times 100\% \tag{6}$$

where SOC_0 is the initial value of the SOC, and C_{bat} denotes the battery rated capacity, i.e., 41 Ah.

In the next step, the ECMS will be employed to achieve real-time energy management of PHEVs.

III. REAL-TIME ENERGY MANAGEMENT STRATEGY

Since the PHEV can be charged from an external power source, the vehicle can be powered only by the motor until the battery SOC drops to an allowable low threshold. In this

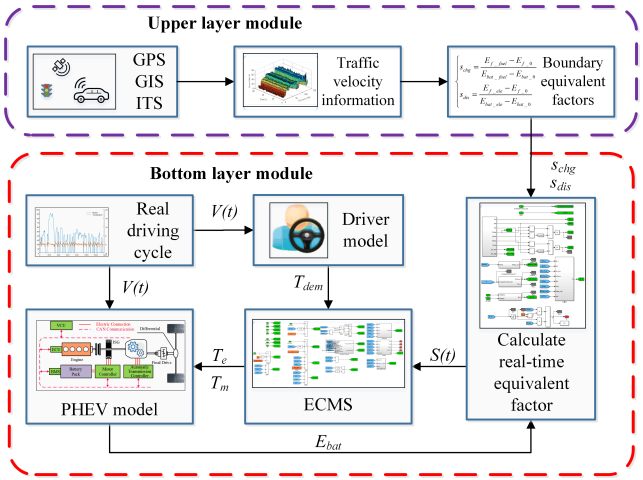

FIGURE 6. Structure of the proposed A-ECMS.

study, the proposed A-ECMS is only applied during the CS stage to manage the energy distribution, thereby achieving superior fuel economy and maintaining the SOC within the designed region. The A-ECMS that is based on the energy balance principle is structured in Fig. 6, from which it can be clearly observed that two control layers exist in the whole framework. Detailed calculation process can be described as follows:

1) Ahead of departure, the global transportation information needs to be acquired with the help of GPS, GIS and ITS, and a pair of boundary equivalent factors can be estimated according to the global driving information.

2) During operation, the equivalent factor is calculated based on the real-time probability factor, which is determined according to variation of the battery energy.

3) By finding the control variables that minimize the Hamilton function, the optimal control target can be optimized and consequently the toque commands of the engine and motor can be determined.

4) Repeat steps 2) to 3) until the vehicle reaches the destination.

A. EQUIVALENT FUEL CONSUMPTION MINIMUM STRATEGY

As is well known, ECMS is a typical energy management strategy for HEVs stemmed from PMP. The essence of ECMS is that the energy released by the battery is transferred to the equivalent fuel consumption, and on this basis, the optimal torque distribution scheme, that can minimize the instantaneous equivalent fuel consumption in the premise of satisfying the driver's demand, is allocated to the engine and motor, respectively.

The overall target of the optimization can be formulated as:

$$F = \min J(u(t), x(t)) \tag{7}$$

where J denotes the fuel consumption, $x(t)$ is the state variable, i.e., the battery SOC, and the engine torque T_e is considered as the control variable $u(t)$. Based on (5) and (6), the following state function can be constructed, as:

$$\dot{x}(t) = f(x(t), u(t), t) = -\frac{I(u(t), E(x), R(x))}{C_{bat}} \tag{8}$$

where $\dot{x}(t)$ denotes the variation rate of the SOC. In addition, x and u are subject to the following constraints,

$$\begin{cases} x_{\min} \le x \le x_{\max} \\ u_{\min} \le u \le u_{\max} \end{cases} \tag{9}$$

Based on (7) and (8),J can be further calculated,

$$J(u, x) = \phi(x(t_f)) + \int_{t_0}^{t_f} \dot{m}_f(u(t), t)dt \tag{10}$$

where $\phi\left(x\left(t_f\right)\right)$ is a penalty term for converging the final SOC to the initial value. In this study, since what we concern is minimization of the fuel consumption during the CS stage, we assume that both the initial SOC and terminal SOC are the same and equal SOC_0. In addition, the main parts of the powertrain are subject to the following constraints, as:

$$\begin{cases} SOC \in (SOC_{\min}, SOC_{\max}) \\ P_{bat} \in (P_{bat\_\min}, P_{bat\_\max}) \\ T_e \in (T_{e\_\min}, T_{e\_\max}) \\ T_m \in (T_{m\_\min}, T_{m\_\max}) \end{cases} \tag{11}$$

where P_{bat} denotes the battery power, and T_m means the motor torque. Here, a co-state variable $\lambda(t)$ is introduced to build the Hamilton function H, as:

$$\begin{aligned} H(x(t), \lambda(t), u(t), t) &= \lambda(t)f(x(t), u(t), t) + \dot{m}_f(u(t), t) \\ &= \lambda(t)\dot{x}(t) + \dot{m}_f(u(t), t) \end{aligned} \tag{12}$$

where $\lambda(t)$ is a time variable, similar to the Lagrange multiplier. According to PMP [31], a necessary condition should be satisfied when minimizing J, as:

$$u^*(t) = \arg\min\left(H(x(t), \lambda(t), u(t), t)\right) \tag{13}$$

where $u^*(t)$ is the optimal control variable. Based on (12), $\dot{\lambda}$ can be derived, as:

$$\dot{\lambda} = -\frac{\partial H(x(t), \lambda(t), u(t), t)}{\partial x(t)} = -\lambda(t)\frac{\partial \dot{x}(t)}{\partial x(t)} \tag{14}$$

Combining (14) and (8), we can attain:

$$\begin{aligned} \dot{\lambda}(t) &= \frac{\lambda(t)}{C_{bat}} \cdot \frac{\partial I(u(t), E(x), R(x))}{\partial x} \\ &= \frac{\lambda(t)}{C_{bat}} \cdot \left(\frac{\partial I}{\partial E} \cdot \frac{\partial E}{\partial x} + \frac{\partial I}{\partial R} \cdot \frac{\partial R}{\partial x}\right) \end{aligned} \tag{15}$$

From (15), we can find that $\lambda(t)$ is highly nonlinear with the battery internal resistance and OCV, thus it is difficult to get an analytical solution. Based on (8), we can get:

$$\dot{x}(t) = \dot{SOC} = -\frac{P_{bat}(t)}{E(SOC) \cdot C_{bat}} \tag{16}$$

By substituting (16) into (12), an updated Hamilton function with respect to $P_{bat}(t)$ can be obtained:

$$H(x(t), s(t), u(t), t) = s(t)\frac{P_{bat}(t)}{H_{LHV}} + \dot{m}_f(t) \tag{17}$$

where $s(t)$ is called the equivalent factor, which can be defined as:

$$s(t) = -\lambda(t)\frac{H_{LHV}}{E(SOC)\cdot C_{bat}} \tag{18}$$

Actually, the physical meaning of $s(t)\frac{P_{bat}(t)}{H_{LHV}}$ in (17) is the equivalent fuel consumption corresponding to the battery power, and we can say that the physical meaning of (17) can be regarded as the current instantaneous equivalent fuel energy consumption. Now the instantaneous equivalent fuel rate $\dot{m}_{equ}$ can be expressed a sum of the fuel rate of the engine $\dot{m}_f$ and equivalent fuel rate of the battery $\dot{m}_{bat}$, as:

$$\dot{m}_{equ}(t) = \dot{m}_{bat}(t) + \dot{m}_f(t) = s(t)\frac{P_{bat}(t)}{H_{LHV}} + \dot{m}_f(t) \tag{19}$$

Based on (13),$u(t)$ can be controlled to minimize $\dot{m}_{equ}(t)$, thereby optimizing the global target function J. For ease of analyzing the energy conversion, the equivalent power consumption $P_{equ}(t)$ can be calculated by multiplying the fuel's lower heat value, as:

$$P_{equ}(t) = s(t)P_{bat}(x, u, t) + P_{fuel}(u, t) \tag{20}$$

where $P_{fuel}(u, t) = \dot{m}_f(t)H_{LHV}$. Now we can consider that the physical meaning of $s(t)$ is the coefficient of transferring the electrochemical energy of the battery to the fuel's lower heat energy.

Based on discussion detailed above, a pivotal problem when applying the ECMS is to decide the equivalent factor properly, which can directly influence the total fuel consumption and driving performance. The larger the equivalent factor, the smaller output power of the electric driving system will be. Under this situation, the energy management strategy tends to reduce the discharge power of the battery or even inversely charge the battery. Or else, if the equivalent factor decreases, the discharge power of the battery will become larger and the motor will provide more power to drive the vehicle. In this manner, the SOC will be controlled within a certain range and can possibly return to its original value at the end of the driving cycle.

In the following, the steps of calculating the equivalent factor based on the energy variation of the powertrain will be detailed.

B. DETERMINATION OF REAL-TIME EQUIVALENT FACTORS

Since the equivalent factor can directly affect management of the engine power and motor power, first, two extreme conditions are herein considered to make sure its searching range can be further restricted: 1) When the engine works with the maximum power output, the vehicle is driven only by the engine and the remaining power is utilized to charge the battery. In this case, remaining energy of the battery is most, and the equivalent factor should be maximum. Now we define it as the charging equivalent factor S_{chg}. 2) When the engine is off and the vehicle is driven purely by the motor, the battery outputs the most energy in comparison with other conditions. In this case, we define the current equivalent factor, which should be minimum, as the discharging equivalent factor S_{dis}. Consequently, we can conclude that $s(t) \in [s_{dis}, s_{chg}]$. For ease of building the relationship among $s(t)$, S_{chg} and S_{dis}, a probability factor $p(t) \in [0, 1]$ is defined, and $s(t)$ can be formulated as:

$$s(t) = p(t)\cdot s_{chg} + (1 - p(t))\cdot S_{dis} \tag{21}$$

Now, the following task turns to determination of S_{chg}, S_{dis}, and $p(t)$.

1) CALCULATION OF THE BOUNDARY EQUIVALENT FACTORS

As discussed above, in order to determine S_{chg} and S_{dis}, we need to first analyze the relationship between the battery energy variation and fuel energy variation. To this end, an energy balance model of the powertrain system is built, and its main function is to describe energy transfer routes when the vehicle operates, as shown in Fig. 7.

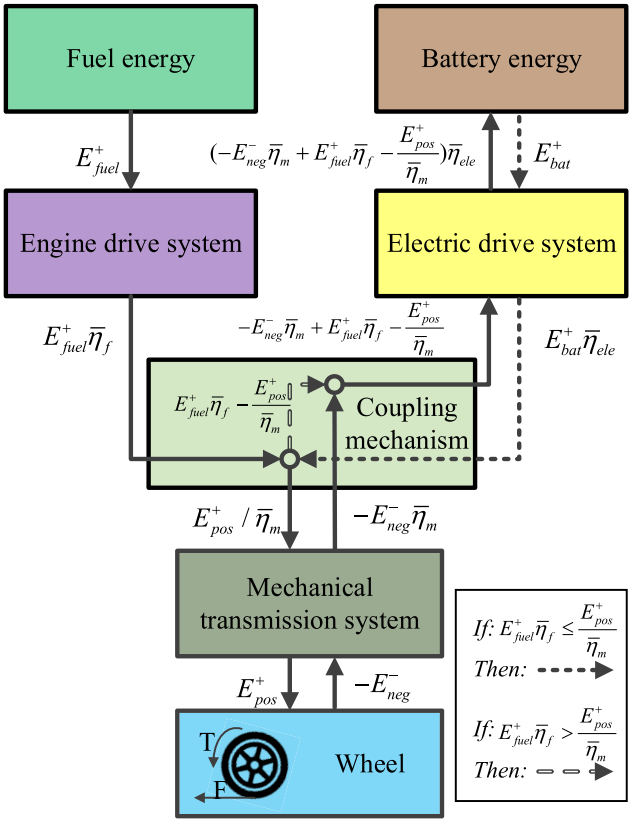

FIGURE 7. The energy balance model of the powertrain system.

As can be seen in Fig. 7, E^+_{fuel} and E^+_{bat} denote the fuel energy and battery energy, and $\bar{\eta}_f$ and $\bar{\eta}_{ele}$ mean the average efficiency of the engine drive system and electric drive system, respectively. E^+_{pos} and E^-_{neg} express the driving energy and regenerative energy, respectively. The regenerative energy stored in the battery can be expressed as $-E^-_{neg} \times \bar{\eta}_m \times \bar{\eta}_{ele}$. When $E^+_{fuel}\bar{\eta}_f \le E^+_{pos}/\bar{\eta}_m$, the engine cannot supply enough driving energy and the battery compensates

the gap with energy of E^+_{bat}; on the contrary, when $E^+_{fuel}\bar{\eta}_f > E^+_{pos}\Big/\bar{\eta}_m$, the engine provides sufficient driving energy and the redundant energy is charged to the battery with energy of $\left(E^+_{fuel}\bar{\eta}_f - E^+_{pos}\Big/\bar{\eta}_m\right)\bar{\eta}_{ele}$.

When the trip ends, the consumed energy of the battery ΔE_{bat} and the fuel energy of the engine ΔE_f can be calculated as:

$$\begin{cases}\Delta E_{bat} = E_{bat\_int} - E_{bat\_end} = \int_0^{t_{end}} \left(E_{OCV}(t)I(t)\right)dt \\ \Delta E_f = H_{LHV}\int_0^{t_{end}} \dot{m}_f(t)dt\end{cases} \tag{22}$$

where E_{bat_int} and E_{bat_end} denote the initial electric energy and remaining energy of the battery, respectively.

If the engine is under the maximum power mode, energy increment of the battery when the trip ends can be calculated as:

$$\Delta E^-_{bat\_fuel} = \left(E^+_{pos}/\bar{\eta}_m - \Delta E^+_{f\_fuel}\times\bar{\eta}_f\right)\times\bar{\eta}_{ele} + E^-_{neg}\times\bar{\eta}_m\times\bar{\eta}_{ele} \tag{23}$$

where $\Delta E^-_{bat\_fuel}$ can be regarded as sum of the regenerative energy and supplemental energy generated from the extra engine power. $\Delta E^+_{f\_fuel}$ is the fuel energy consumption that partially drives the vehicle and meanwhile residually powers the motor for charging the battery.

Similarly, if the vehicle is under the pure electrical driving mode, the consumed energy when the trip ends can be calculated as:

$$\Delta E^+_{bat\_ele} = \left(E^+_{pos}/\bar{\eta}_m - \Delta E^+_{f\_ele}\times\bar{\eta}_f\right)/\bar{\eta}_{ele} + E^-_{neg}\times\bar{\eta}_m\times\bar{\eta}_{ele} \tag{24}$$

where $\Delta E^+_{bat\_ele}$ denotes the difference between the driving energy from the battery and regenerative braking energy, and $\Delta E^+_{f\_ele}$ denotes the consumed fuel energy in this mode. To calculate S_{chg} and S_{dis}, another special condition needs to be considered, in which the engine power equals the driving power and the regenerative energy is utilized to charge the battery. Now, we can attain:

$$\begin{cases}\Delta E^-_{bat\_0} = E^-_{neg}\times\bar{\eta}_m\times\bar{\eta}_{ele} \\ \Delta E^+_{f\_0}\times\bar{\eta}_f\times\bar{\eta}_m = E^+_{pos}\end{cases} \tag{25}$$

where $\Delta E^-_{bat\_0}$ denotes the energy stored in the battery from regeneration, $\Delta E^+_{f\_0}$ indicates fuel energy of the engine in this condition. By substituting (25) into (23) and (24) and eliminating E^+_{pos} and E^-_{neg}, the relationship between the fuel energy and battery energy under these two extreme conditions can be obtained, as:

$$\begin{cases}\left(\Delta E^-_{bat\_0} - \Delta E^-_{bat\_fuel}\right)\times\dfrac{1}{\bar{\eta}_f\bar{\eta}_{ele}} = \Delta E^+_{f\_fuel} - \Delta E^+_{f\_0} \\ \left(\Delta E^-_{bat\_0} - \Delta E^+_{bat\_ele}\right)\times\dfrac{\bar{\eta}_{ele}}{\bar{\eta}_f} = \Delta E^+_{f\_ele} - \Delta E^+_{f\_0}\end{cases} \tag{26}$$

As discussed in Section III, the physical meaning of $s(t)$ is the coefficient when the battery electrochemical energy is converted into the lower fuel heat energy of the engine. As such, $1/\left(\bar{\eta}_f\bar{\eta}_{de}\right)$, expressed in (26), denotes the value of s_{chg} when the engine supplies the maximum output power; and $\bar{\eta}_{ele}/\bar{\eta}_f$ indicates the values of s_{dis} when the vehicle is under the pure electric driving mode. Consequently, s_{dis} and s_{dis} can be calculated, as:

$$\begin{cases}s_{chg} = \dfrac{1}{\bar{\eta}_f\bar{\eta}_{ele}} = \dfrac{\Delta E^+_{f\_fuel} - \Delta E^+_{f\_0}}{\Delta E^-_{bat\_0} - \Delta E^-_{bat\_fuel}} \\ s_{dis} = \dfrac{\bar{\eta}_{ele}}{\bar{\eta}_f} = \dfrac{\Delta E^+_{f\_ele} - \Delta E^+_{f\_0}}{\Delta E^-_{bat\_0} - \Delta E^+_{bat\_ele}}\end{cases} \tag{27}$$

Now, we can conclude that based on (26) and (27), S_{chg} and S_{dis} can be determined by analyzing the fuel consumption and battery status under these three extreme conditions.

2) DETERMINATION OF THE INSTANTANEOUS PROBABILITY FACTOR

After calculating these two boundary equivalent factors, $p(t)$ needs to be determined. Here we suppose that the maximum discharging energy and maximum charging energy of the battery are respectively $E^+_{s_{dis}}(t)$ and $E^-_{s_{chg}}(t)$ from the current moment until the end of the trip. In order to ensure that the ending SOC equals with the initial value, we attain:

$$[SOC_0 - SOC(t)]\times C_{bat}\times E_{OCV} + E^-_{s_{chg}}(t)\times p(t) + E^+_{s_{dis}}(t)\times[1-p(t)] = 0 \tag{28}$$

where SOC_0 denotes the initial SOC, and $SOC(t)$ is the current SOC. Based on (28), the probability factor can be calculated,

$$p(t) = \frac{E^+_{s_{dis}}(t) + [SOC_0 - SOC(t)]\times C_{bat}\times E_{OCV}(t)}{E^+_{s_{dis}}(t) - E^-_{s_{chg}}(t)} \tag{29}$$

It is necessary to note that in order to guarantee adaptive regulation of the probability factor according to the driving condition, $E^+_{s_{dis}}(t)$ and $E^-_{s_{chg}}(t)$ should be updated in real time. To attain it, we divided them into three parts: 1) the currently consumed battery energy E_{now}; 2) the regenerative energy E^-_{re} absorbed from the motor in the remaining trip; and 3) the released energy $E^+_{e_dis}$ or absorbed energy $E^-_{e_chg}$ of the battery in the remaining trip when $S = S_{dis}$ or $S = S_{chg}$. As such, we can get,

$$\begin{cases}E^+_{s_{dis}}(t) = E_{now} + E^-_{re} + E^+_{e\_dis} \\ E^-_{s_{chg}}(t) = E_{now} + E^-_{re} + E^-_{e\_chg}\end{cases} \tag{30}$$

where E_{now} can be calculated by integrating the real-time power, as:

$$E_{now} = \int_0^t E_{OCV}(t)I(t)dt \tag{31}$$

In addition, the regenerative energy E^-_{re} can be calculated,

$$E^-_{re} = \Delta E^-_{bat\_0} - \Delta E^-_{bat\_0}(t) \tag{32}$$

Furthermore, the released energy $E^{+}_{e\_dis}$ and absorbed energy $E^{-}_{e\_chg}$ can be determined, as:

$$\begin{cases} E^{+}_{e\_dis} = \dfrac{\left[E^{+}_{pos} - E^{+}_{pos}(t)\right]}{\bar{\eta}_{ele}\bar{\eta}_{m}} \\ E^{-}_{e\_chg} = \bar{\eta}_{ele}\left\{\bar{\eta}_{f}\left[\Delta E^{+}_{f\_fuel} - \Delta E^{+}_{f\_fuel}(t)\right] - \dfrac{\left[E^{+}_{pos} - E^{+}_{pos}(t)\right]}{\bar{\eta}_{m}}\right\} \end{cases} \tag{33}$$

Combining (25) and (27), we can calculate these three efficiency coefficients, as:

$$\begin{cases} \bar{\eta}_{ele} = \sqrt{s_{dis}/s_{chg}} \\ \bar{\eta}_{f} = 1/\sqrt{s_{dis}s_{chg}} \\ \bar{\eta}_{m} = E^{+}_{pos}/\left(E^{+}_{f\_0}\bar{\eta}_{f}\right) \end{cases} \tag{34}$$

Now based on (29)–(34), $p(t)$ can be determined. Then, according to the determined s_{chg} and s_{dis} together with $p(t)$, the real-time equivalent factor trajectories can be sequentially determined. In the next step, simulation is conducted to calculate the equivalent factor, apply the proposed ECMS strategy and demonstrate its efficacy.

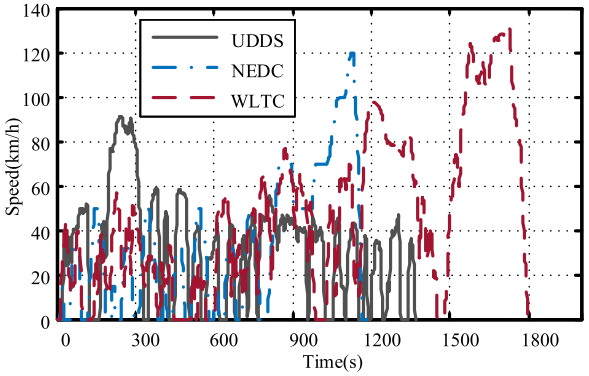

FIGURE 8. Speed curve of three driving cycles.

IV. SIMULATION AND DISCUSSIONS

To verify performance of the proposed real-time energy management strategy, simulations were carried out based on Autonomie, which is an effective and precise vehicle simulation tool developed by Argonne National Laboratory [32]. Since the battery degrades gradually with usage and the driving conditions are possibly acquired with some error, in this study, we divide the whole simulation into three parts: 1) study with healthy battery, 2) study with the degraded battery, and 3) validation with inaccurate global driving condition. As such, the algorithm adaptivity can be substantially validated. In this paper, three typical driving cycles, i.e., UDDS, NEDC and WLTC, were simulated to compare the fuel savings with respect to the proposed A-ECMS and traditional ECMS. Corresponding speed profiles of these three driving cycles are shown in Fig. 8, demonstrating that the vehicle speed profile includes the highway and the urban condition.

TABLE 2. The best equivalent factor of UDDS, NEDC and WLTC.

Driving cycle	Value
UDDS	$s_{UDDS} = 3.37$
NEDC	$s_{NEDC} = 3.79$
WLTC	$s_{WLTC} = 3.27$

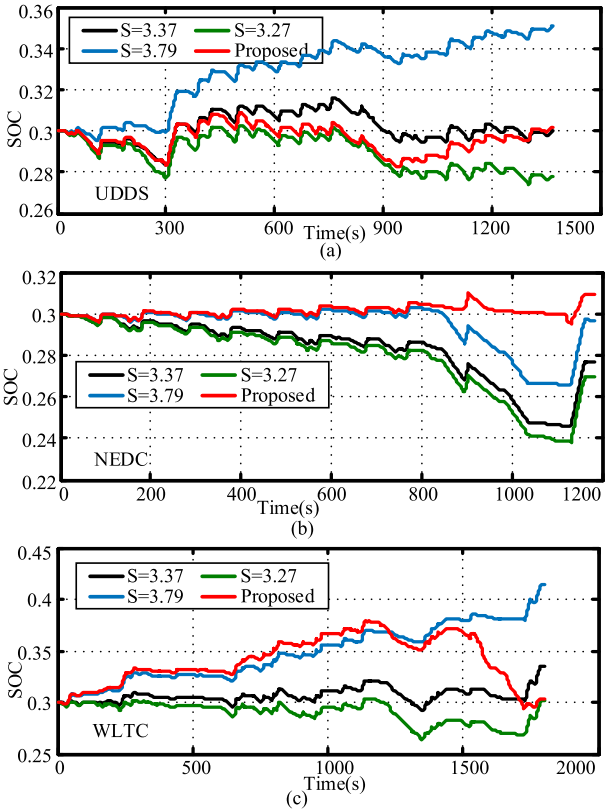

FIGURE 9. SOC curves of two algorithms under three driving cycles. (a) UDDS cycle; (b) NEDC cycle; (c) WLTC cycle.

A. COMPARING THE PROPOSED ALGORITHM WITH TRADITIONAL ECMS UNDER DIFFERENT DRIVING CYCLES

In this study, two indicators are applied to evaluate performances of the proposed control strategy, of which one is the fuel consumption in the end of the trip and the other is the final SOC value. We assume that the initial SOC equals 0.3, which means the vehicle certainly operates in the CS stage. After a variety of trial and error, the optimal equivalent factors, i.e., S_{UDDS}, S_{NEDC} and S_{WITC}, under these three driving cycles can be found for the typical ECMS, as listed in Table 2. Then, we apply each parameter to realize the energy management of PHEVs under these three cycles. All the nine SOC variation curves in comparison with those based on the proposed algorithm are shown in Fig. 9. To fairly compare fuel savings, a fuel consumption correction technique,

TABLE 3. Simulation results of two algorithms under three typical driving cycles.

		UDDS			NEDC			WLTC		
		SOC	FC (kg)	CFC (kg)	SOC	FC (kg)	CFC (kg)	SOC	FC (kg)	CFC (kg)
ECMS	$s = 3.37$	0.300	0.5074	0.5074 (+0.61%)	0.277	0.4028	0.5175 (-14.47%)	0.335	1.093	1.022 (+0.78%)
	$s = 3.79$	0.351	0.6227	0.5122 (-0.33%)	0.297	0.4493	0.4643 (-4.67%)	0.414	1.278	1.048 (-1.72%)
	$s = 3.27$	0.278	0.4607	0.5558 (-8.15%)	0.269	0.3848	0.5394 (-17.94%)	0.301	1.018	1.016 (+1.38%)
Proposed strategy		0.302	0.5148	0.5105	0.309	0.4620	0.4426	0.303	1.036	1.030

Note: +: Increment; -: Reduction

formulated in (34), is applied to make sure that the ending SOC is the same.

$$CFC = FC - \frac{\Delta SOC \times W_{SOC} \times \bar{\eta}_{ele}^{sgn(\Delta SOC)}}{\bar{\eta}_{lf} \times H_{LHV} \times 1000} \tag{35}$$

where CFC means the corrected fuel consumption, FC expresses the fuel consumption, $\Delta SOC = SOC_{ead} - SOC_{\text{int}}$ denotes the difference between the final SOC and target SOC, and W_{soc} indexes the whole energy that could be released by the battery, as:

$$W_{SOC} = 3.6 \times 72 \times 41 \times 3600\ (J) \tag{36}$$

According to (35) and (36), the corrected fuel consumption results are listed in Table 3. From Fig. 9, it can be observed that the proposed A-ECMS can maintain the ending SOC in the vicinity of the setting value, however, the traditional EMCS can only guarantee that the optimal equivalent factor corresponding to the current driving cycle can maintain the ending SOC value as desired and may lead to obvious drift if the unmatched equivalent factor is applied to the current driving cycle. By comparing the corrected fuel consumption listed in Table 3, the proposed algorithm can achieve more fuel savings than the traditional ECMS. For instance, under the UDDS cycle, when the equivalent factor of the traditional ECMS equals to the optimal equivalent factor s_{UDDS}, the corresponding fuel saving is 0.61% more than that based on the proposed algorithm. However, if the equivalent factor is not equal to the optimal factor calculated based on the current driving profile and instead equals the optimal factor based on the NEDC or WLTC cycle, the fuel saving of the traditional ECMS will be worse than that of the proposed algorithm. In contrast, the adopted A-ECMS algorithm can dynamically regulate the equivalent factor according to the driving condition, thereby ensuring the superior fuel economy all the time.

B. ADAPTATION BEHAVIOR OF PROPOSED STRATEGY WITH DEGRADED BATTERY PARAMETERS

Since the proposed algorithm determines S_{dis} and S_{chg} in terms of the energy balance function before departure, the battery health status, that reflects the battery energy variation, will lead to change of the boundary equivalent factors. Thus, the real-time equivalent factor should be updated accordingly. Existing research reveals that when the

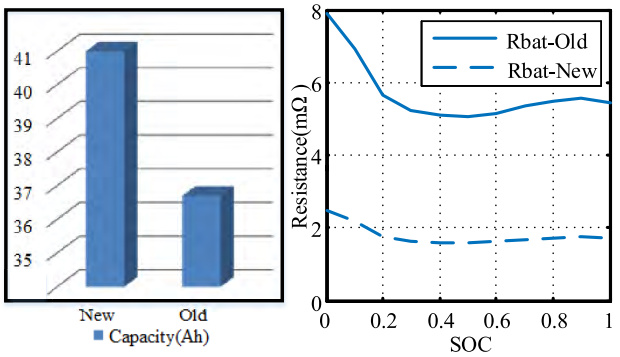

FIGURE 10. Battery parameters comparison.

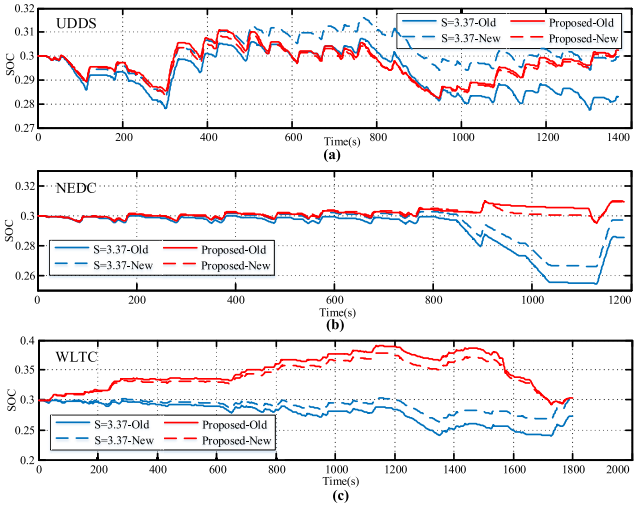

FIGURE 11. SOC curves based on the two algorithms with the degraded battery under three driving cycles. (a) UDDS cycle. (b) NEDC cycle. (c) WLTC cycle.

battery degrades, the capacity decreases, the internal resistance increases, and yet the OCV does not show obvious change [33], [34]. According to the degradation data supplied in [35], in this study, we suppose that the battery capacity drops from 41 Ah to 36.7 Ah after 1900 cycles. The capacity variation and resistance increment are shown in Fig. 10. As before, three driving cycles are simulated based on the proposed A-ECMS and the traditional ECMS, respectively, and both algorithms consider the battery capacity variation. Related results are shown in Figs. 11–12 and listed

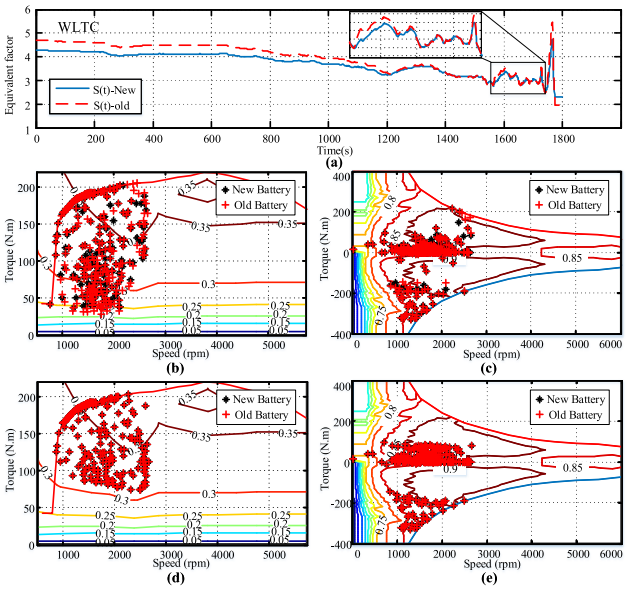

FIGURE 12. Simulation results based on the two algorithms with degraded battery parameters under the WLTC cycle. (a) Equivalent factor curve based on the proposed algorithm. (b) Engine operating point based on the proposed algorithm. (c) Motor operating point based on the proposed algorithm. (d) Engine operating point based on the traditional ECMS. (e) Motor operating point based on the traditional ECMS.

TABLE 4. Comparison of the boundary equivalent factors with different battery parameters under three driving cycles.

	UDDS		NEDC		WLTC	
	s_{dis}	s_{chg}	s_{dis}	s_{chg}	s_{dis}	s_{chg}
New battery	2.50	4.98	2.48	5.72	2.32	6.24
Old battery	2.25	5.36	2.21	6.17	1.94	6.78

TABLE 5. Battery efficiency comparison with degraded and healthy battery under three driving cycles.

	UDDS		NEDC		WLTC	
	New	Old	New	Old	New	Old
ECMS	0.9870	0.9559	0.9886	0.9688	0.9848	0.9559
Proposed strategy	0.9867	0.9639	0.9930	0.9810	0.9866	0.9634

in Tables 4-6. Fig. 11 depicts the SOC curves based on the two algorithms under three driving cycles. Fig. 12 shows the trajectory of the equivalent factor under the WLTC cycle, and the operating points of the engine and motor based on the two algorithms. Table 4 compares the boundary equivalent factors with different health status of the battery. To conveniently compare and analyze two algorithms, the average operating efficiency of the battery is listed in Table 5 and corresponding fuel consumption is demonstrated in Table 6.

From Fig. 11, it can be found that the SOC trajectory based on the proposed strategy is kept almost the same with that of the healthy battery. Nevertheless, since the equivalent factor of the traditional ECMS is fixed, the SOC trajectory when the battery is degraded differs obviously from that when the battery is healthy, and the ending SOC under the degraded condition deviates from the setting 0.3. As can be found in Table 4, when the battery parameters change after degradation, the proposed A-ECMS can dynamically update the boundary equivalent factors, and the charging equivalent factor s_{chg} increases, whilst the discharging equivalent factor s_{dis} decreases. As can been illustrated in Fig. 12 (a), due to variations of the boundary equivalent factors, the real-time equivalent factor based on the proposed algorithm changes accordingly, thereby guaranteeing that the ending SOC maintains near the initial setting value.

As shown in Fig. 12 (b)-(e), it can also be observed that in order to maintain the SOC near the initial value, the operating points of the engine and motor vary obviously. As mentioned before, when the battery capacity degrades, its internal resistance increases. To reduce the energy lost dissipated by the internal resistance during driving, the motor operating points will move downward on a large scale, meaning that the motor power and bus current will decrease when driving the vehicle; and to ensure that enough regenerative power can be absorbed, the motor operating points remain basically the same as before when the vehicle decelerates. In this case, the output power of the engine needs to increase to compensate the gap caused by the motor, thereby meeting requirement of the driving demand. From Table 6, we can find that when the simulation is conducted with the traditional ECMS based on the degraded battery, the fuel consumption is the same as that based on the healthy battery, however, the ending SOC becomes lower. This is because the traditional ECMS still adopts the previous optimal equivalent actor, which keeps the operating properties of the engine and battery almost unchanged, the ending SOC exhibits obvious drop caused by the internal resistance increment and capacity attenuation.

As can be seen in Table 5, when the battery degrades, its operating efficiency would certainly decrease due to increase of the internal resistance, and accordingly the proposed algorithm adaptively reduces the motor power and improves the engine power. In this manner, the battery internal energy loss can be reduced, and thus the proposed algorithm regulates the battery power output with higher efficiency, compared to that of the traditional ECMS. As such, the fuel savings can be further improved. From Table 6, we can find that the proposed A-ECMS is much more superior than the traditional ECMS when the battery degrades. The corrected fuel savings can reach up to 5% to 11%, proving self-adaptivity and robustness of the proposed algorithm.

C. PERFORMANCE ANALYSIS UNDER THE CONDITION OF INACCURATE ROAD INFORMATION

In this study, an assumption is made that the whole road conditions can be acquired in advance based on GPS, GIS and ITS. However, precise acquisition is not an easy task. Usually, the anticipated global driving information is estimated by calculating the average speed of vehicles on road

TABLE 6. Simulation results of two algorithms with degraded or healthy battery parameters under three driving cycles.

	UDDS				NEDC				WLTC			
	$s_{UDDS}=3.37$		Proposed strategy		$s_{NEDC}=3.79$		Proposed strategy		$s_{WLTC}=3.27$		Proposed strategy	
	New	Old	New	Old	New	Old	New	Old	New	Old	New	Old
SOC	0.300	0.283	0.302	0.302	0.297	0.285	0.309	0.309	0.301	0.273	0.303	0.303
FC(kg)	0.5074	0.5074	0.5148	0.5452	0.4493	0.4493	0.4620	0.4778	1.018	1.0180	1.036	1.1020
CFC(kg)	0.5074	0.5782 (-6.31%)	0.5105	0.5417	0.4643	0.5212 (-11.30%)	0.4426	0.4623	1.016	1.1606 (-5.45%)	1.030	1.0974

Note：+: Increment; -: Reduction

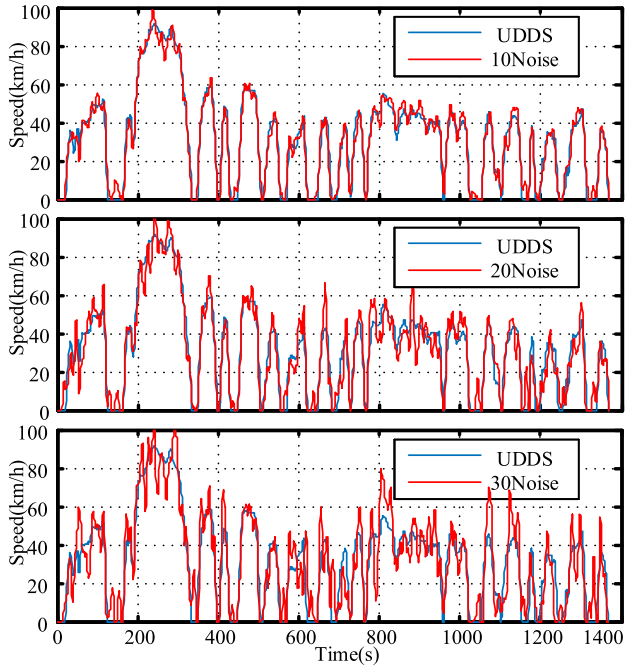

FIGURE 13. The speed profiles with different noises.

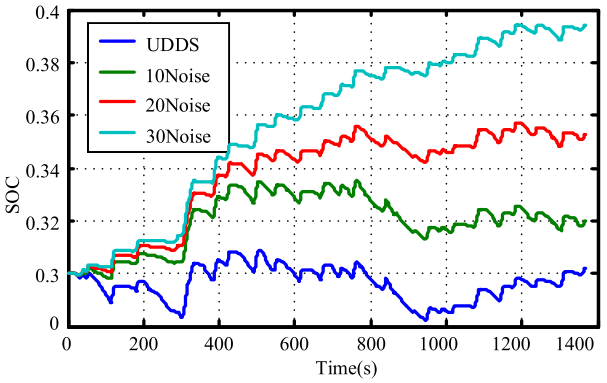

FIGURE 14. The SOC trajectories with differences of driving conditions.

TABLE 7. Simulation results with different noise of driving conditions.

	UDDS	10Noise	20Noise	30Noise
RMSE	0	3.75	7.12	10.94
s_{chg}	4.98	6.68	7.78	10.9
s_{dis}	2.50	2.42	2.33	2.22
SOC	0.302	0.32	0.353	0.394
FC (kg)	0.5148	0.5533	0.629	0.7324
CFC (kg)	0.5105	0.5110	0.5217	0.5517

within certain intervals [36, 37]. Thus, some difference may exist between the real vehicle speed and statistical average speed. To further validate the fuel savings when acquiring the global driving condition with different errors, the UDDS is adopted and the white noise with amplitudes of 10, 20 and 30 is respectively added. Then, a one-order lowpass filter is imposed to smooth the vehicle speed profile. In this manner, the new driving condition with certain errors is generated, as shown in Fig. 13.

As depicted in Fig. 13, the 10Noise, 20Noise and 30Noise denote the updated driving cycles which are processed by the lowpass filter after adding the white noises with amplitudes of 10, 20 and 30, respectively. As can be seen, the vehicle speed varies more obviously than before, and the root-mean square error (RMSE) between the constructed driving cycle and original cycle is 3.75, 7.12 and 10.94, respectively. Related simulations were conducted, the SOC variation curves are shown in Fig. 14 and detailed results are listed in Table 7.

As presented in Table 7, when the RMSE of the constructed driving cycle becomes larger, the charging boundary equivalent factor will increase, and the discharging boundary equivalent factor will decrease. This is arisen by large fluctuation of the vehicle speed when the noise is added. From Fig. 14, we can find that when the 10Noise cycle is simulated, the SOC trajectory is similar with that based on the original UDDS cycle; and when the RSME becomes larger, the SOC trajectory derivates more obviously from the setting 0.3. From Table 7, we find that the corrected fuel consumption of the 10Noise cycle is almost the same as that of the original UDDS cycle; however, when the RMSE becomes larger, the fuel consumption greatly increases. To summarize, we can say that large speed errors would certainly lead to increment of the fuel consumption, and when there exists limited difference between the acquired road information and real driving speed, the proposed algorithm can still take effect in saving the fuel consumption.

V. CONCLUSION

In this paper, a novel A-ECMS is proposed to achieve the energy management of PHEVs during the CS stage. To achieve it, the global speed information is acquired ahead

of departure, and a real-time varied probability factor and a pair of boundary equivalent factors are dynamically determined according to the energy balance function and battery status. Then, the equivalent factor is adaptively regulated according to the global information and boundary equivalent factors. Based on it, the proposed A-ECMS finalizes the energy distribution of the target PHEV in real time. Simulation results manifest the effectiveness and self-adaptivity of the proposed A-ECMS, in particular when the battery capacity degrades and when inaccurate road information is acquired.

Next step work will be focused on improving the fuel economy further by refining control parameters. In addition, the hardware-in-the-loop (HIL) validation and actual vehicle test will also be conducted based on the proposed algorithm.

REFERENCES

[1] C. Mi and M. A. Masrur, *Hybrid Electric Vehicles: Principles and Applications with Practical Perspectives*. Hoboken, NJ, USA: Wiley, 2017.

[2] M. F. M. Sabri, K. A. Danapalasingam, and M. F. Rahmat, "A review on hybrid electric vehicles architecture and energy management strategies," *Renew. Sustain. Energy Rev.*, vol. 53, pp. 1433–1442, Jan. 2016.

[3] Z. Chen, N. Guo, J. Shen, R. Xiao, and P. Dong, "A hierarchical energy management strategy for power-split plug-in hybrid electric vehicles considering velocity prediction," *IEEE Access*, vol. 6, pp. 33261–33274, 2018.

[4] S. Onori, L. Serrao, and G. Rizzoni, *Hybrid Electric Vehicles: Energy Management Strategies*. Berlin, Germany: Springer, 2016.

[5] S. G. Wirasingha and A. Emadi, "Classification and review of control strategies for plug-in hybrid electric vehicles," *IEEE Trans. Veh. Technol.*, vol. 60, no. 1, pp. 111–122, Jan. 2011.

[6] J. Peng, H. He, and R. Xiong, "Rule based energy management strategy for a series–parallel plug-in hybrid electric bus optimized by dynamic programming," *Appl. Energy*, vol. 185, pp. 1633–1643, Jan. 2017.

[7] B. V. Padmarajan, A. McGordon, and P. A. Jennings, "Blended rule-based energy management for PHEV: System structure and strategy," *IEEE Trans. Veh. Technol.*, vol. 65, no. 10, pp. 8757–8762, Oct. 2016.

[8] A. Rezaei, J. B. Burl, M. Rezaei, and B. Zhou, "Catch energy saving opportunity in charge-depletion mode, a real-time controller for plug-in hybrid electric vehicles," *IEEE Trans. Veh. Technol.*, vol. 67, no. 11, pp. 11234–11237, Nov. 2018.

[9] R. Xiong, J. Cao, and Q. Yu, "Reinforcement learning-based real-time power management for hybrid energy storage system in the plug-in hybrid electric vehicle," *Appl Energy*, vol. 211, pp. 538–548, Feb. 2018.

[10] S. Xie, X. Hu, S. Qi, and K. Lang, "An artificial neural network-enhanced energy management strategy for plug-in hybrid electric vehicles," *Energy*, vol. 163, pp. 837–848, Nov. 2018.

[11] H. Liu, X. Li, W. Wang, L. Han, and C. Xiang, "Markov velocity predictor and radial basis function neural network-based real-time energy management strategy for plug-in hybrid electric vehicles," *Energy*, vol. 152, pp. 427–444, Jun. 2018.

[12] Y. Huang *et al.*, "A review of power management strategies and component sizing methods for hybrid vehicles," *Renew. Sustain. Energy Rev.*, vol. 96, pp. 132–144, Nov. 2018.

[13] T. Liu, H. Yu, H. Guo, Y. Qin, and Y. Zou, "Online energy management for multimode plug-in hybrid electric vehicles," *IEEE Trans. Ind. Inform.*, to be published.

[14] S.-Y. Chen, C.-H. Wu, Y.-H. Hung, and C.-T. Chung, "Optimal strategies of energy management integrated with transmission control for a hybrid electric vehicle using dynamic particle swarm optimization," *Energy*, vol. 160, pp. 154–170, Oct. 2018.

[15] R. Xiao, B. Liu, J. Shen, N. Guo, W. Yan, and Z. Chen, "Comparisons of energy management methods for a parallel plug-in hybrid electric vehicle between the convex optimization and dynamic programming," *Appl. Sci.*, vol. 8, no. 2, p. 218, 2018.

[16] N. Guo, J. Shen, R. Xiao, W. Yan, and Z. Chen, "Energy management for plug-in hybrid electric vehicles considering optimal engine ON/OFF control and fast state-of-charge trajectory planning," *Energy*, vol. 163, pp. 457–474, Nov. 2018.

[17] C.-C. Lin, H. Peng, J. W. Grizzle, and J.-M. Kang, "Power management strategy for a parallel hybrid electric truck," *IEEE Trans. Control Syst. Technol.*, vol. 11, no. 6, pp. 839–849, Nov. 2003.

[18] P. Elbert, T. Nüesch, A. Ritter, N. Murgovski, and L. Guzzella, "Engine ON/OFF control for the energy management of a serial hybrid electric bus via convex optimization," *IEEE Trans. Veh. Technol.*, vol. 63, no. 8, pp. 3549–3559, Oct. 2014.

[19] Z. Chen, C. C. Mi, R. Xiong, J. Xu, and C. You, "Energy management of a power-split plug-in hybrid electric vehicle based on genetic algorithm and quadratic programming," *J. Power Sour.*, vol. 248, no. 15, pp. 416–426, Feb. 2014.

[20] B.-H. Nguyen, R. German, J. P. F. Trovao, and A. Bouscayrol, "Real-time energy management of battery/supercapacitor electric vehicles based on an adaptation of Pontryagin's minimum principle," *IEEE Trans. Veh. Technol.*, vol. 68, no. 1, pp. 203–212, Jan. 2019.

[21] P. Zhang, F. Yan, and C. Du, "A comprehensive analysis of energy management strategies for hybrid electric vehicles based on bibliometrics," *Renew. Sustain. Energy Rev.*, vol. 48, pp. 88–104, Aug. 2015.

[22] S. Zhang, R. Xiong, and F. Sun, "Model predictive control for power management in a plug-in hybrid electric vehicle with a hybrid energy storage system," *Appl. Energy*, vol. 185, pp. 1654–1662, Jan. 2017.

[23] J. Han, Y. Park, and D. Kum, "Optimal adaptation of equivalent factor of equivalent consumption minimization strategy for fuel cell hybrid electric vehicles under active state inequality constraints," *J. Power Sour.*, vol. 267, pp. 491–502, Dec. 2014.

[24] C. M. Martinez, X. Hu, D. Cao, E. Velenis, B. Gao, and M. Wellers, "Energy management in plug-in hybrid electric vehicles: Recent progress and a connected vehicles perspective," *IEEE Trans. Veh. Technol.*, vol. 66, no. 6, pp. 4534–4549, Jun. 2017.

[25] C. Sun, F. Sun, and H. He, "Investigating adaptive-ECMS with velocity forecast ability for hybrid electric vehicles," *Appl. Energy*, vol. 185, pp. 1644–1653, Jan. 2017.

[26] Z. Chen, B. Xia, C. You, and C. C. Mi, "A novel energy management method for series plug-in hybrid electric vehicles," *Appl. Energy*, vol. 145, pp. 172–179, May 2015.

[27] Y. Zeng, Y. Cai, G. Kou, W. Gao, and D. Qin, "Energy management for plug-in hybrid electric vehicle based on adaptive simplified-ECMS," *Sustainability*, vol. 10, no. 6, p. 2060, 2018.

[28] S. Onori and L. Tribioli, "Adaptive pontryagin's minimum principle supervisory controller design for the plug-in hybrid GM chevrolet volt," *Appl. Energy*, vol. 147, pp. 224–234, Jun. 2015.

[29] J. T. B. A. Kessels, M. W. T. Koot, P. P. J. van den Bosch, and D. B. Kok, "Online energy management for hybrid electric vehicles," *IEEE Trans. Veh. Technol.*, vol. 57, no. 6, pp. 3428–3440, Nov. 2008.

[30] K. M. Alam, M. Saini, and A. E. Saddik, "Toward social Internet of vehicles: Concept, architecture, and applications," *IEEE Access*, vol. 3, pp. 343–357, 2015.

[31] D. Liberzon, *Calculus of Variations and Optimal Control Theory: A Concise Introduction*. Princeton, NJ, USA: Princeton Univ. Press, 2011.

[32] N. Kim, A. Rousseau, and E. Rask, "Autonomie model validation with test data for 2010 toyota prius," SAE, Pennsylvania, PA, USA, Tech. Paper 0148-7191, 2012.

[33] S. Schwunk, N. Armbruster, S. Straub, J. Kehl, and M. Vetter, "Particle filter for state of charge and state of health estimation for lithium–iron phosphate batteries," *J. Power Sour.*, vol. 239, no. 10, pp. 705–710, 2013.

[34] S. F. Schuster, M. J. Brand, C. Campestrini, M. Gleissenberger, and A. Jossen, "Correlation between capacity and impedance of lithium-ion cells during calendar and cycle life," *J. Power Sour.*, vol. 305, pp. 191–199, Feb. 2016.

[35] W. Waag, S. Käbitz, and D. U. Sauer, "Experimental investigation of the lithium-ion battery impedance characteristic at various conditions and aging states and its influence on the application," *Appl. Energy*, vol. 102, no. 2, pp. 885–897, 2013.

[36] A. Nantes, D. Ngoduy, A. Bhaskar, M. Miska, and E. Chung, "Real-time traffic state estimation in urban corridors from heterogeneous data," *Transp. Res. C, Emerg. Technol.*, vol. 66, pp. 99–118, May 2016.

[37] J. C. Herrera, D. B. Work, R. Herring, X. Ban, Q. Jacobsond, and A. M. Bayen, "Evaluation of traffic data obtained via GPS-enabled mobile phones: The mobile century field experiment," *Transp. Res. C, Emerg. Technol.*, vol. 18, no. 4, pp. 568–583, Aug. 2010.

YONGGANG LIU received the B.S. and Ph.D. degrees in automotive engineering from Chongqing University, Chongqing, China, in 2004 and 2010, respectively.

He was a joint Ph.D. Student and a Research Scholar with the University of Michigan–Dearborn, MI, USA, from 2007 to 2009. He is currently a Professor and a Dean Assistant with the School of Automotive Engineering, Chongqing University. He has leaded more than ten research projects and has published more than 40 research journal papers. His research interests mainly include optimization and control of intelligent electric and hybrid vehicles, and integrated control of vehicle automatic transmission system. He is also a Committee Member of Vehicle Control and Intelligence Society of the Chinese Association of Automation (CAA).

JIE LI received the B.S. degree in mechanical engineering from Anhui University, Hefei, China, in 2017. He is currently pursuing the M.S. degree in mechanical engineering with Chongqing University, Chongqing, China.

His research is mainly focused on optimal control and energy management for hybrid electric vehicles.

ZHENZHEN LEI received the M.S. degree in automotive system engineering from the University of Michigan–Dearborn, USA, in 2009. She is currently pursuing the Ph.D. degree with Chongqing University, Chongqing, China.

She is also a Lecturer of mechanical and power engineering with the Chongqing University of Science and Technology, Chongqing. She has published more than15 peer-reviewed journal papers and conference proceedings. Her research interests include energy management of plug-in hybrid electric vehicles and optimal control of intelligent electric vehicles.

WENZHI LI received the B.S. degree in mechanical engineering from Liaoning Technical University, Fuxin, China, in 2016. He is currently pursuing the M.S. degree in vehicle engineering with Chongqing University, Chongqing, China.

His research is focused on the energy management strategy and adaptive cruise control of plug-in hybrid electric vehicles.

DATONG QIN received the B.S., M.S., and Ph.D. degrees in mechanical engineering from Chongqing University, Chongqing, China, in 1982, 1984, and 1993, respectively.

In 1989, he was a joint Ph.D. Student with Tohoku University, Sendai, Miyagi, Japan. He is currently a Professor with the State Key Laboratory of Mechanical Transmissions and the School of Automotive Engineering, Chongqing University, Chongqing, China. He has conducted more than 60 projects and has published more than 200 peer-reviewed journal papers and conference proceedings. His research interests include control and application of mechanical transmission and vehicle power transmission. He was a recipient of the Changjiang Scholars Program of China and the two first prizes of provincial-level scientific and technological progress awards, in 2008 and 2010.

ZHENG CHEN received the B.S. and M.S. degrees in electrical engineering and the Ph.D. degree in control science engineering from Northwestern Polytechnical University, Xi'an, China, in 2004, 2007, and 2012, respectively.

He is currently a Professor with the Faculty of Transportation Engineering, Kunming University of Science and Technology, Kunming, Yunnan, China. He was a Postdoctoral Fellow and a Research Scholar with the University of Michigan–Dearborn, Dearborn, USA, from 2008 to 2014. He has conducted more than 20 projects and has published more than 80 peer-reviewed journal papers and conference proceedings. His research interests include battery management systems, battery status estimation, and energy management of hybrid electric vehicles. He was a recipient of the Yunnan Oversea High Talent Project, China, and received the Second Place of the IEEE VTS Motor Vehicles Challenge, in 2017 and 2018.